Hindawi
Geofluids
Volume 2023, Article ID 9207960, 11 pages
https://doi.org/10.1155/2023/9207960

Research Article

Provenance and Tectonic Setting Discrimination and Their Effects on the Pore-Scale Fluid Flow of Black Shale: Take the Micangshan Tectonic Belt, Central China, as an Example

Tao Tian,[1,2] **Jianming Yao**,[3] **Wenxiang Guo**,[2] **Zhonghui Duan**,[1,3] **Deliang Fu**,[1,3] **and Fu Yang**[1,3]

[1]*Key Lab of Coal Resources Exploration and Comprehensive Utilization, MNR, Xi'an, China*
[2]*Shaanxi Coal Geology Oil & Gas Drilling Co., Ltd., Xi'an, China*
[3]*Shaanxi Coal Geology Group Co., Ltd., Xi'an, China*

Correspondence should be addressed to Tao Tian; tiantao870211@163.com

Received 2 September 2022; Revised 26 December 2022; Accepted 18 March 2023; Published 21 April 2023

Academic Editor: Wenhui Li

The Lower Paleozoic reservoir in the Micangshan tectonic belt is a new shale gas exploration area with excellent potential. However, the black shale's sedimentary environment and tectonic setting and their effects on pore-scale fluid flow have not been thoroughly elucidated and urgently require further research. A large amount of trace and rare earth element data of black shale in this area was tested to analyze the sediment's provenance, tectonic setting, and coupling process, and nuclear magnetic resonance was applied for fluid flow ability determination. The characteristics of trace elements and rare earth elements in shale samples were drilled from the Upper Sinian Doushantuo Formation, the Lower Cambrian Niutitang Formation, and the Lower Silurian Longmaxi Formation in the Micangshan tectonic belt. The results reveal that the provenance of the shales was dominated by island arc volcanic rocks and some ancient fine-grained sediments. The provenances of shale in the Micangshan, Huijunba, and Zhenba areas may have a strong genetic relationship with the igneous rocks from the nearest Hannan massif. The provenance of the Niutitang shale in the Ningqiang area may comprise sediments derived from the Longmenshan continental rift system. The provenance of the shale tends to transition from the island arc to the continental margin from the depositional stage of the Doushantuo Formation to the Longmaxi Formation. The Micangshan tectonic belt inherited the tectonic evolution of the South China block, North China block, and Qinling, and those blocks provided the igneous provenance of the shale by island arcs, which were formed due to weathering caused by the process of subduction and collision orogeny. The movable fluid distribution of the Longmaxi Formation and Niutitang Formation is relatively uniform, and excessive pursuit of large amount of movable fluid will be counterproductive to the shale reservoir. The proportion of the cracks was generally less than 3% except for one sample from the Doushantuo Formation with 12.06%. Based on the centrifugation force in this research, the low fluid flow limits were less than 1.47, and there are strong positive relationships between movable fluid saturation and saturated porosity. In this study, the coupling relationship between the material source and pore scale flow is discussed for the first time, and the results can provide theoretical references for local provenance analysis and tectonic movement.

1. Introduction

The Lower Paleozoic shales, especially for the Lower Silurian Longmaxi Formation (LSLF) and Lower Cambrian Niutitang Formation (LCNF) in the Sichuan basin and its peripheral regions, such as the Upper Sinian Doushantuo Formation (USDF), are important strata for the breakthrough of marine shale gas exploration in South China [1–4]. In recent years, substantial shale gas has been found in the LCNF, and the latest research suggests that the Lower Cambrian and Neoproterozoic shale in the Micangshan tectonic belt (MTB) may contain new and ideal

exploration target reservoirs [5–8]. The development of organic-rich shale is the material basis for shale gas accumulation, and the sedimentary environment plays an important role in preserving and enriching organic matter [9–13]. However, the MTB is in the transitional area between the Sichuan basin and the Qinling orogenic belt (QOB), resulting in distinctive geological conditions which are more complex than other shale gas exploration areas. Therefore, the understanding of the sedimentary and tectonic environment of black shale is of great significance for guiding future shale gas in the MTB.

The geochemical properties of trace elements (TE) and rare earth elements (REE) are extremely stable and were hardly modified by tectonic activities and diagenesis [14]. Some TE and REE preserved in the clastic rocks record the tectonic environment information of the source area [15]. Therefore, based on the above characteristics, TE and REE are commonly used to trace the parent rock of sedimentary rocks, the nature of sedimentary basins, and the tectonic setting [16–22].

In order to develop the shale gas economically and efficiently, the determination of the fluid flow behavior is important [23]. Nuclear magnetic resonance is a typical method for the fluid ability calculation, and it has been used in many fields. The T_1 and T_2 relaxation times before and after the sample centrifugation would determine the movable fluid saturation, and other vital parameters could be calculated through related formulas.

In this study, a large number of TE and REE data were acquired to analyze the sediment's provenance, tectonic setting, and coupling process of black shale in the LSLF, LCNF, and USDF in the MTB, and typical samples were selected for the purpose of nuclear magnetic resonance conduction. Based on the above experimental procedures, this research has three main objectives: (1) to analyze the nature of shale source rocks, (2) to determine the tectonic movement behaviors, and (3) to calculate the fluid flow ability. The purposes of this study are to provide theoretical and technical support for provenance and tectonic movement in the study area and reveal the coupling relationships between them and the pore-scale fluid flow behavior.

2. Methods

2.1. Geological Setting. The MTB is located at the junction of the QOB and Sichuan basin (Figure 1(a)), a passive continental margin formed in the early Paleozoic [24, 25]. At the beginning of the late Caledonian, the South China block (SCB) was subducted under the North China block (NCB) [26]. This movement led to full collision until the Late Triassic and experienced continuous compression as well as reconstruction in the Yanshan-Himalayan [26]. Finally, the thrust nappe structure, thrust faults, and continuous fold deformation were formed and were widely distributed [4, 26–29]. Three sets of black shale formations of the LSLF, LCNF, and USDF were formed and strongly reformed by multiple tectonic processes (Figures 1(b)–1(d)). The lithology of the shale samples is mainly composed of black carbonaceous shale, organic-rich siliceous shale, and organic silty shale.

2.2. Samples and Methods. A total of 173 samples were selected for TE and REE analyses. The measured shale samples of LSLF, LCNF, and USDF were collected from the field outcrop sections and gas well in the Ningqiang area (NA), Huijunba syncline (HJS), Micangshan massif (MM), and eastern Zhenba area (EZA) (Figure 1). Before the tests, all samples were oil washed to avoid element determination typos. And then, samples were dried at the temperature of 60°C. There is no specific criterion for shales; therefore, the methods which have been used for silica rocks were introduced. RE and REE tests were completed at the National Research Center of Geoanalysis, China, using a PE300Q Plasma mass spectrometer according to the "Methods for Chemical Analysis of Silicate Rocks—Part 30: Determination of 44 Elements" (GB/T 14506.30-2010) enacted by Standardization of the People's Republic of China. The samples were first separated and then placed into the cables. All calculation methods were based on the criterion of GB/T 14506.30-2010. The nuclear magnetic resonance (NMR) tests were done using a Niumag Portable Nuclear Magnetic Resonance device. The latency time, echo spacing, number of scans, and number of echoes were set at 6 s, 0.2 ms, 64, and 18,000, respectively. Dried cores were scanned initially to prevent errors. And then, the T_2 relaxation times before and after centrifugation were measured, and the centrifugation force was 1.44 MPa.

3. Results

In this research, we focused on three types of shale: Longmaxi shale, Niutitang shale, and Doushantuo shale. For the purpose of detailed analysis, the shales in different regions were analyzed separately. Therefore, eight groups of the samples were analyzed: Longmaxi shale in northeast and eastern Micangshan; Niutitang shale in Ningqiang, eastern and northeast Micangshan, Haojunba, and Zhenba; and Doushantuo shale in eastern Zhenba. Previous well-logging results show that Longmaxi and Niutitang shales have relatively high production targets, so this research mainly focuses on those shales.

3.1. Trace Element Results. In this study, the diagrams, such as La/Th-Hf, Co/Th-La/Sc, La/Yb-REE, and Th-Hf-Co, were used to analyze the nature of shale source rocks in the MTB [19, 21, 30–35]. The data from different areas and strata were demonstrated from Table S1 to Table S8. On the plot of La/Th against Hf (Figure 2(a)), most data fall in the acidic arc source field and cluster around the field of the upper continental crust. Meanwhile, a few samples fall in mixed felsic/basic source regions and others, indicating an increasing composition of old sediment. In the Co/Th against La/Sc diagram (Figure 2(b)), the data show a low and relatively constant Co/Th ratio as well as a high and variable La/Sc ratio, which suggests that the source rocks of the shale were dominantly felsic volcanic rocks. However, the data of LCNF shale in the NA show a much lower Co/Th ratio which indicates that the provenance of LCNF shale in this area was different from others. In the

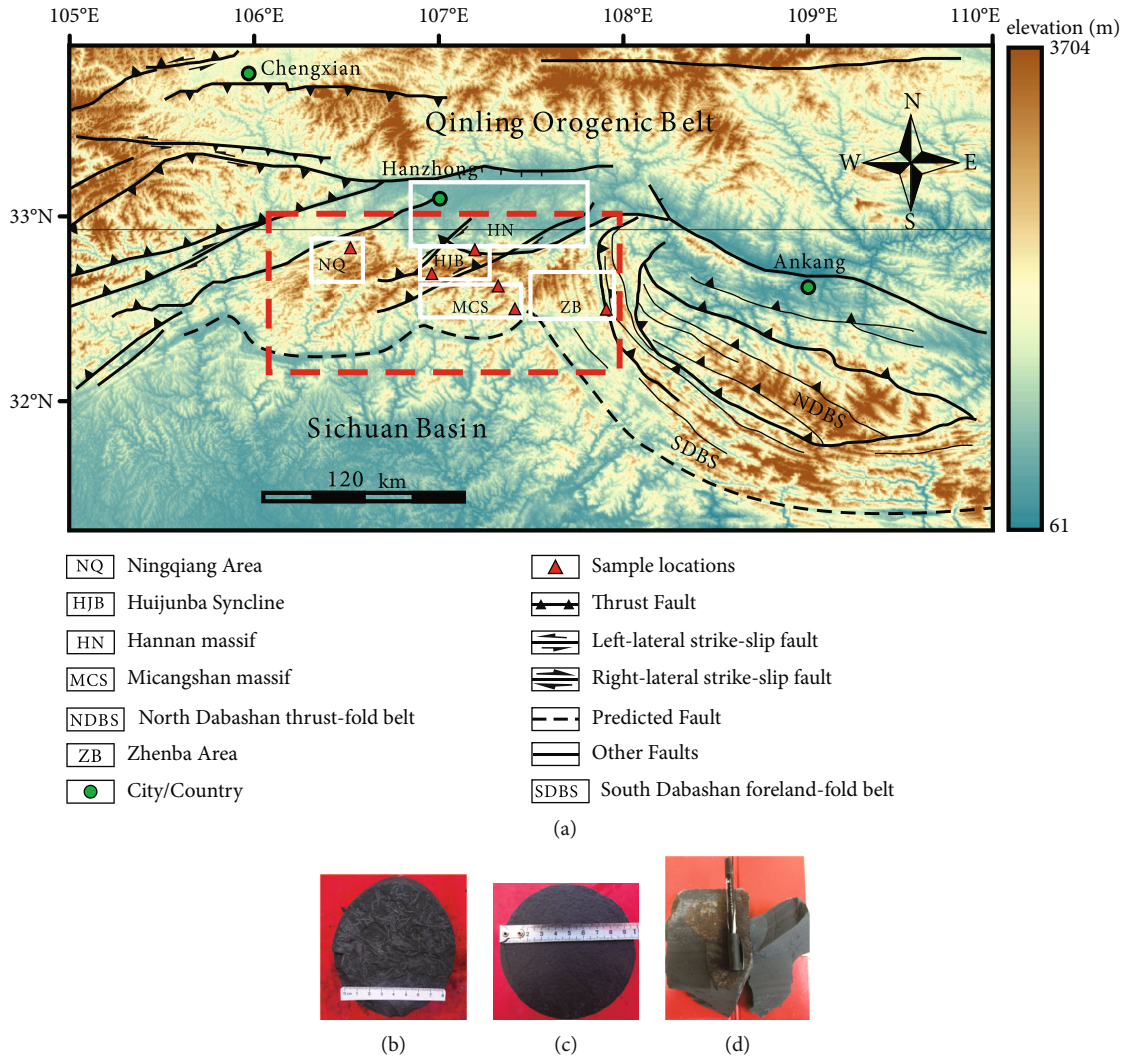

Figure 1: (a) Geological sketch map of the study area and sampling location; (b) black carbonaceous shale of Longmaxi Formation with graptolites; (c) black carbonaceous shale of Niutitang Formation; (d) silty shale of Doushantuo Formation.

La/Yb against ∑REE diagram (Figure 2(c)), sample points are concentrated in the overlaps of alkaline basalt, granite, and calcareous sedimentary rock, which indicate the diversity of shale sedimentary material sources in the study area. As Figure 2(d) shows, abundant data were distributed near the Th-Hf-Co regions, which indicated that most samples of LSLF and LCNF shale in the MM, HJS, and EZA fell into the fields of felsic volcanic rocks and shale. However, the LCNF shale samples in the NA area fell into the field of arkose which is quite different from other shales.

3.2. Rare Element Results. In the La-Th-Sc, Th-Co-Zr/10, and Th-Sc-Zr/10 plots [30], most data fall into the fields of the continental island arc (Figures 3(b) and 3(c)), whereas few LSLF and LCNF shale samples fall into the active continental arc or passive margin regions (Figure 3(a)). It shows that the tectonic setting of different shales was composed of the continental island arc, passive continental margin, active continental margin, and mutual transformation.

3.3. Nuclear Magnetic Resonance Results. In this study, two typical samples were selected for the NMR T_2 spectrum analysis according to the horizon. The results show that the saturated fluid content of the Longmaxi Formation and Niutitang Formation is relatively high, and the saturated fluid content of the Doushantuo Formation is quite different. The saturated fluid heterogeneity of the Doushantuo Formation is strong, and the saturated fluid of the same horizon in different areas is quite different, indicating that the evaluation of the recoverable degree in this area is relatively complex. Both the Longmaxi Formation and Niutitang Formation are highly saturated samples, and the overall hydrocarbon saturation is relatively high.

The samples before and after centrifugation can be used to evaluate the collectability (Figure 4). On the whole, the recoverable degree of this area is relatively low, and the recoverable degree and the initial saturation basically belong to a parallel relationship; that is, the higher the initial saturation, the higher the recoverable degree. At the same time, the recoverable degree of large pores is relatively high, and the strong seepage capacity of fractures can provide important support for recovery.

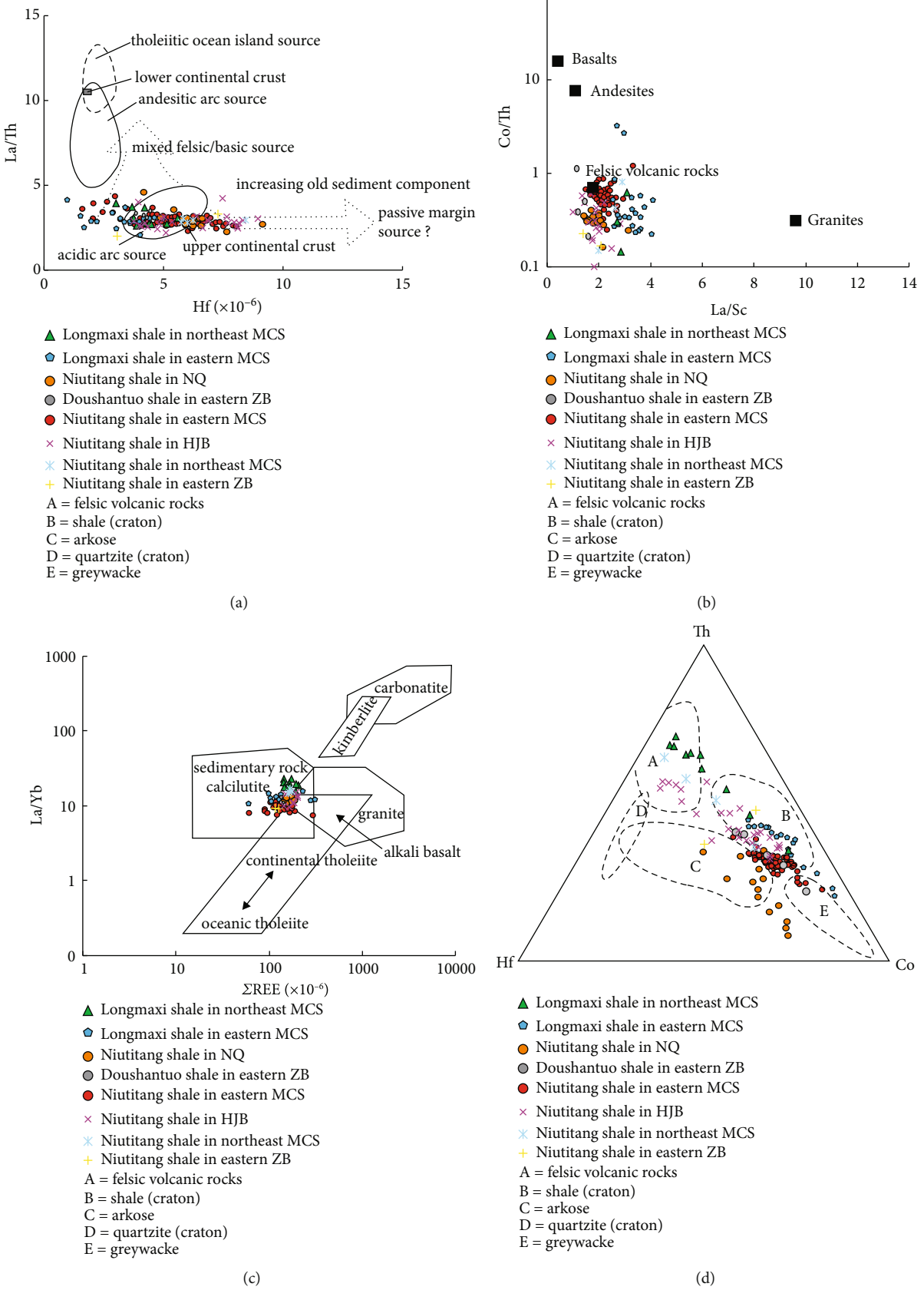

Figure 2: Discrimination diagrams illustrating sedimentary provenance of shale in Micangshan tectonic belt. (a) La/Th against Hf diagram (after [32]); (b) Co/Th against La/Sc diagram (after [34]); (c) La/Yb against REE diagram (after [36]); (d) Th-Hf-Co diagram (after [31]).

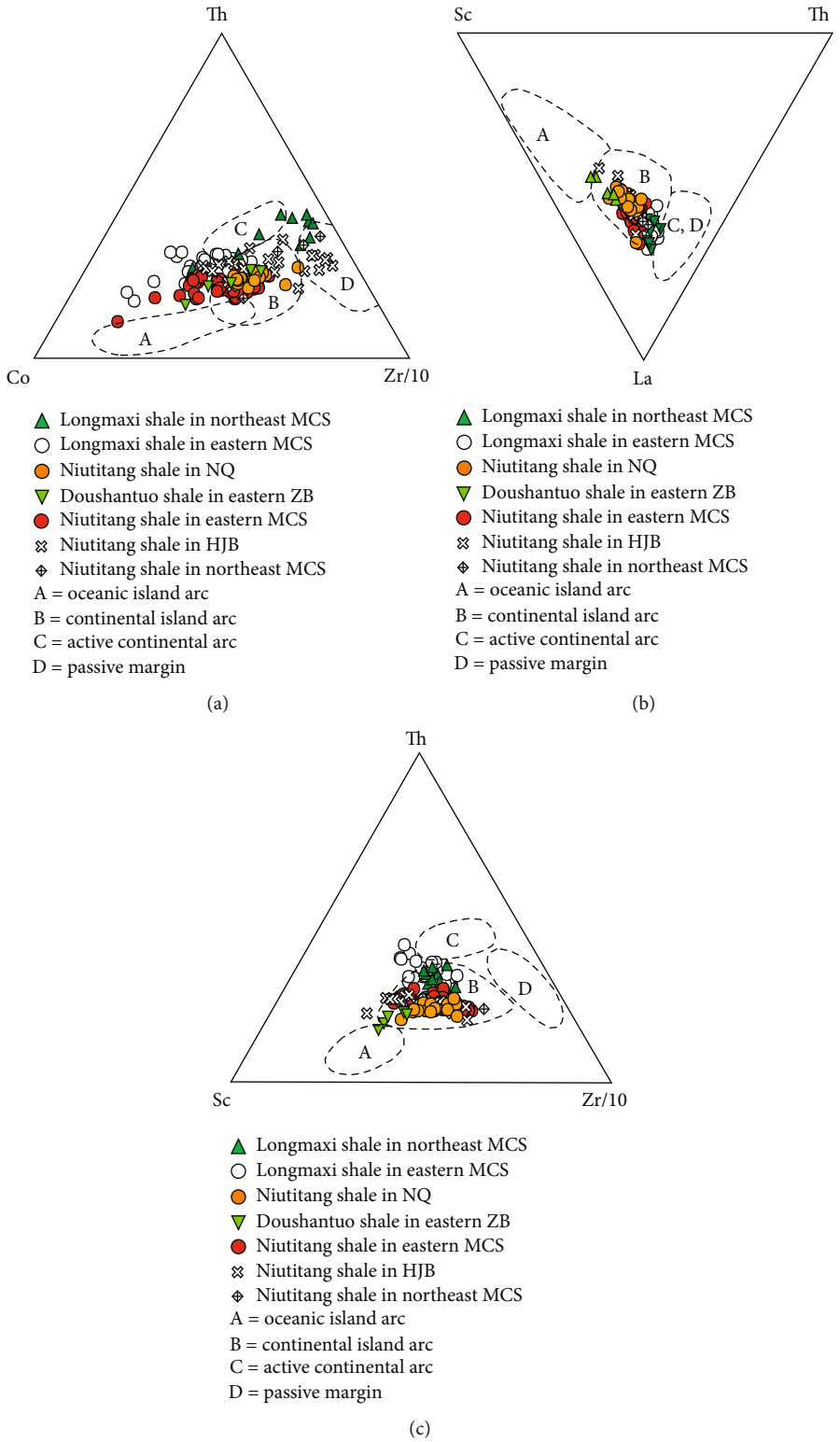

Figure 3: Th-Co-Zr/10 (a), La-Th-Sc (b), and Th-Sc-Zr/10 (c) plots of shale for tectonic discrimination.

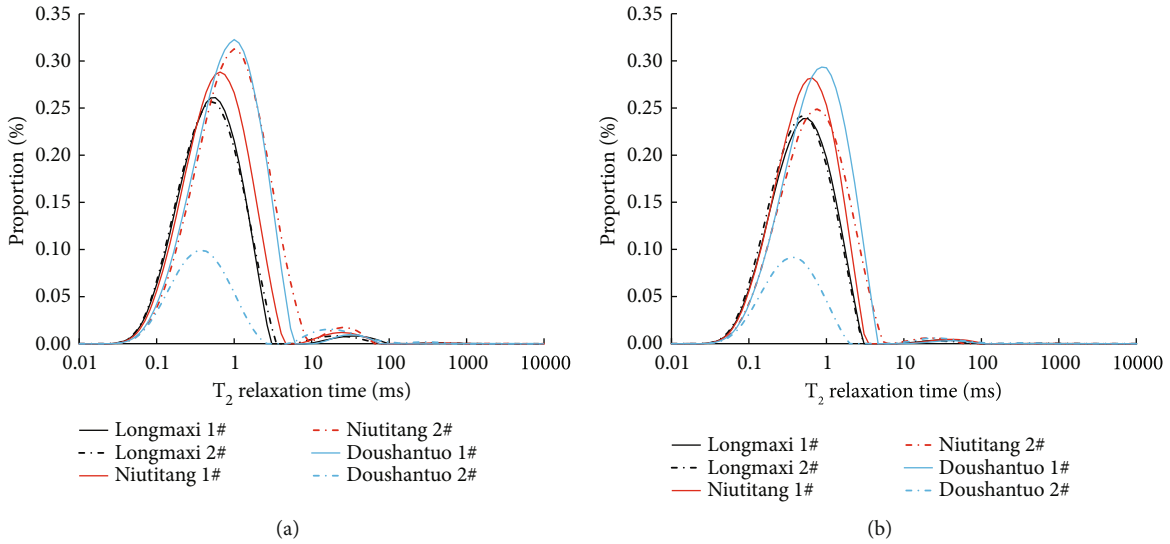

Figure 4: T_2 spectra for (a) before and (b) after centrifugation.

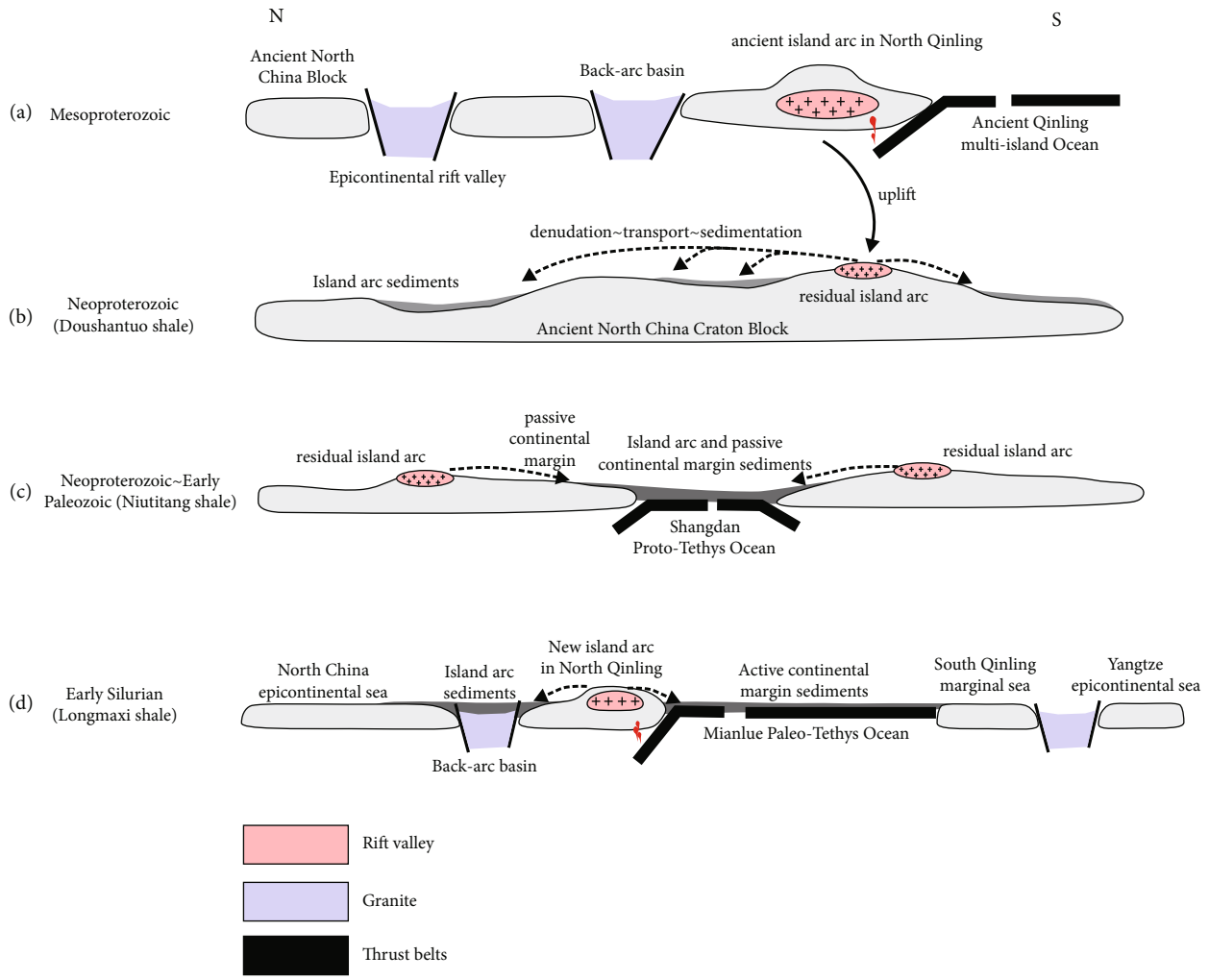

Figure 5: The relationships between the sediment's provenance and tectonic setting of shale. (a) Mesoproterozoic, (b) Neoproterozoic, (c) Neoproterozoic-Early Paleozoic, and (d) Early Silurian.

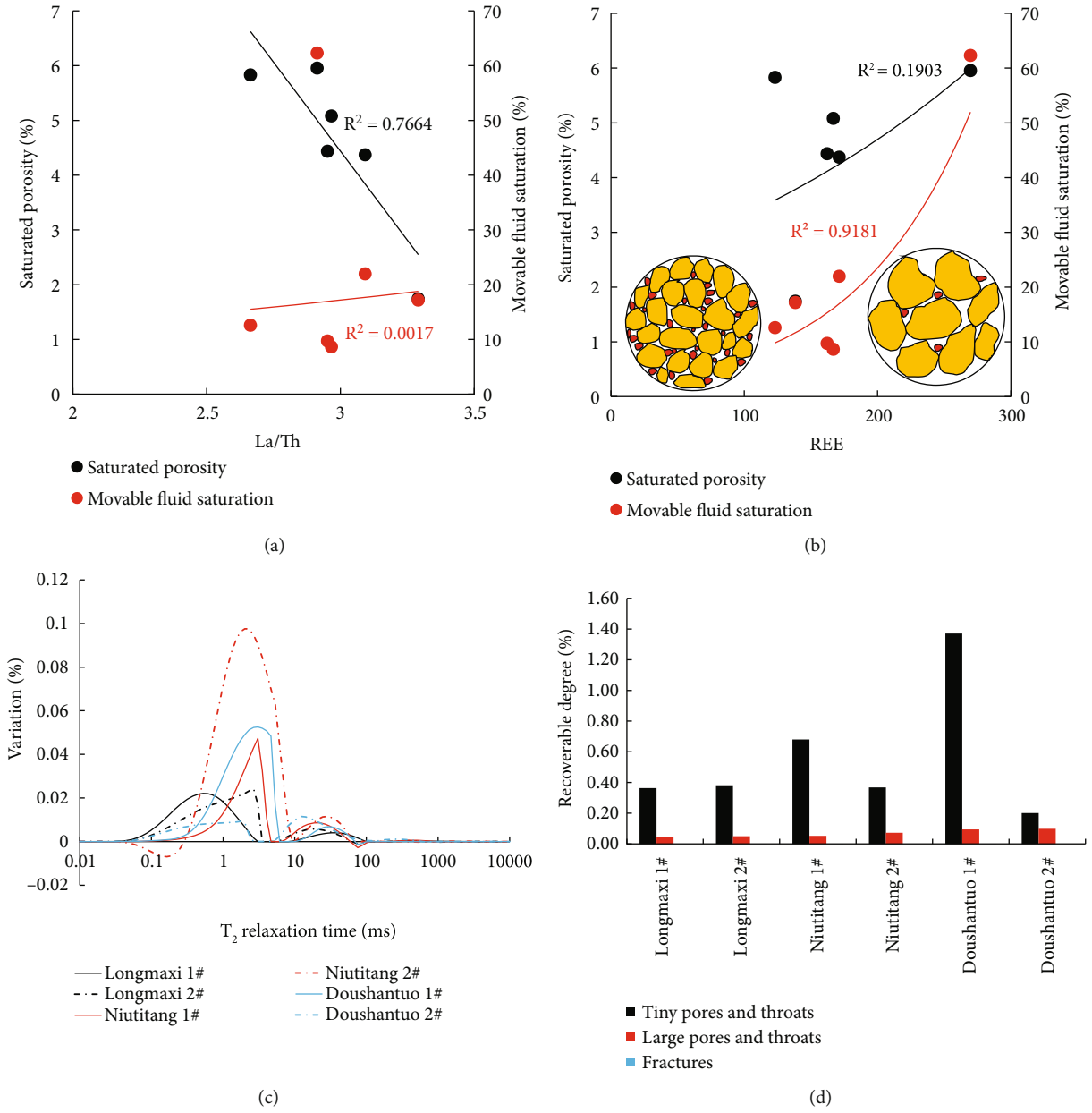

FIGURE 6: The relationships between (a) La/Th and saturated porosity and movable fluid saturation, (b) REE and saturated porosity and movable fluid saturation, (c) recoverable degree distributions, and (d) recoverable degree in the different research areas.

4. Discussion

4.1. Nature of Shale Source Rocks. TE and REE were generally not affected by weathering, transport, and deposition; hence, the information derived from them could usually reflect the parent rock completely [17, 18, 30]. The elements, such as Th and La, are relatively enriched in felsic rock, while Co, Sc, and Cr have very high content in basic rock [18]. Therefore, discrimination diagrams of these characteristic elements can be used for the analysis of rock provenance [18]. The discrimination diagrams illustrating sedimentary provenance of the shale above indicate that the shale provenances in MTB were felsic volcanic rocks and old sedimentary rocks. The provenance of felsic volcanic rocks may be mainly from the Hannan massif (HN) rather than the MM, because the latter was an underwater uplift before the Late Triassic. The sedimentation restricted its contribution and cannot provide sources for the LSLF and LCNF shales [8, 24, 37]. The provenance of LCNF shale in the NQ area may comprise sediments derived from the Longmenshan continental rift system (LCRS). LSLF deposits accepted both passive continental margin and active continental margin as well as island arc provenance (Figure 2).

4.2. Tectonic Setting. The distinctive elemental compositions of clastic rocks in different tectonic environments have been widely used to indicate the tectonic setting of sedimentary basins [18]. The relationship between tectonic setting and geochemical processes gives a deeper understanding of

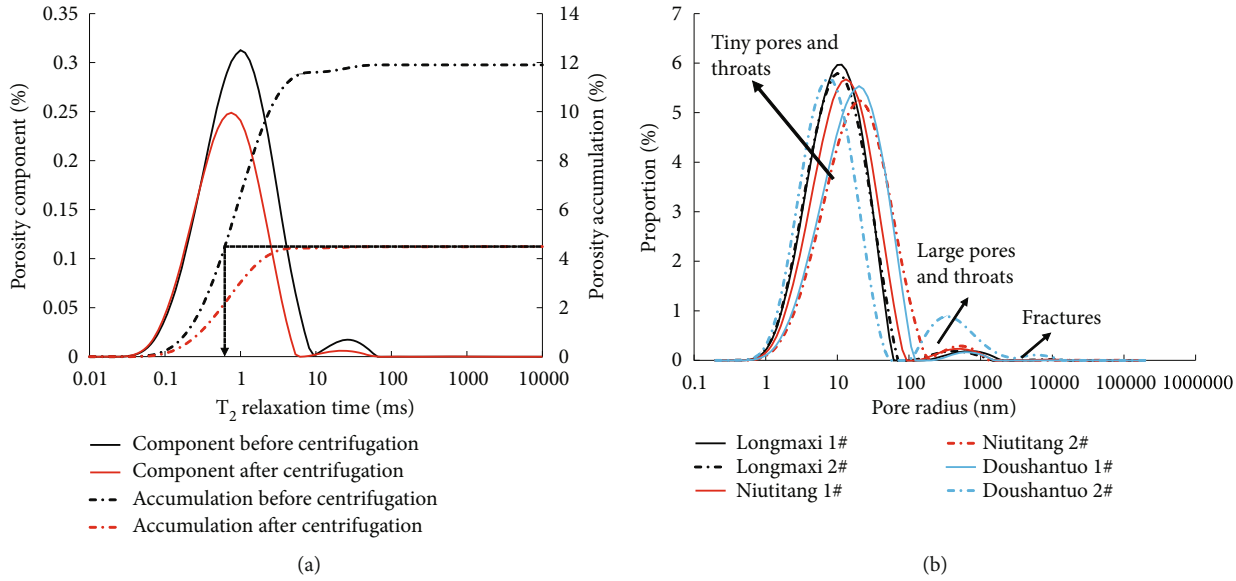

Figure 7: (a) Transformation method of T_2 value to pore throat; (b) pore radius distributions.

tectonics and sediment compositions [34, 35, 38, 39]. The sedimentary tectonic setting was gradually variable from USDF to LSLF; it started as the continental island arc, then converted to the passive continental margin, and, finally, evolved to the active continental margin.

The geochemical process is consistent with the regional tectonic background in the MTB. In the Mesoproterozoic, the study area entered the plate tectonic system, and the ancient continent split and formed the intercontinental ancient Qinling multi-island ocean [40]. The Jinning Movement brought the multicontinent block together with collision orogeny in the north and subduction orogeny in the south. Then, the "ancient" island arc was formed during the orogenic process (Figure 5(a)). After that, the Qinling ocean closed, and the NCB and the SCB converged for the first time during the Late Mesoproterozoic to the Early Neoproterozoic [41, 42]. In the Early Sinian, USDF was a stable cratonic deposit in the ancient continent of North China, and the EZA was a plate inland surface sea deposit. The "ancient" island arc in the North Qinling experienced weathering and then was denuded, which provided the provenance for USDF shale (Figure 5(b)). For the same reason, the provenance was inherited in the continental island arc, and the parent rock was mainly felsic acidic volcanic rock (Figure 2). The North China Supercontinent split and dispersed at the end of Sinian and formed the Proto-Tethys Ocean. Since then, the SCB and the NCB began different types of continental margin evolution (Figure 5(c)) [4, 27, 43]. In the Early Cambrian, the study area was the passive continental margin, and the LCNF shale had passive continental margin and "ancient" continental island arc provenance (Figure 2). In the Early Silurian, SCB began to undergo subduction to the NCB from the passive continental margin to the active continental margin. Finally, a "new" island arc was formed in the Northern Qinling (Figure 5(d)).

4.3. Effects of Nature of Sources on Pore-Scale Fluid Flow. La/Th and REE are two important indicators to evaluate the provenance system. The previous research shows that this area belongs to the ocean land island mixed transition zone, so high La/Th indicates abundant oceanic crust material sources and less continental crust material sources, and high REE indicates shallow water sedimentary units. As shown in Figures 6(a) and 6(b), for the study area, the high oceanic crust material contributes little to the overall saturated porosity, and the rich continental crust material source is an important guarantee for the high gas saturation. Figures 6(c) and 6(d) indicate the recoverable degree. It is found that the material source is not the most important indicator affecting the recoverable degree. However, the shallow water sedimentary unit has relatively small porosity due to the relatively strong hydrodynamic force and small particles that are difficult to preserve, but the seepage channel is relatively wide and the recoverable degree is relatively high.

4.4. Effects of Nature of Sources on Low Fluid Flow Limits. The T_2 spectrum can be converted into the pore throat radius, and a certain amount of data processing is required before that. As shown in Figure 7(a), the cumulative spectra before and after centrifugation are counted first, and then, the curve after centrifugation is inversely extended. The T_2 data corresponding to the point where the curve intersects with the curve before centrifugation is the T_2 cutoff value. The space corresponding to the right of the T_2 cutoff value is the fluid space. The total proportion of the fluid space is taken as the pore volume, and then, its T_2 value is converted into the pore throat radius. As shown in Figure 7(b), all samples are dominated by the pore throat-type reservoir space, with few microfractures and fractures in the Longmaxi Formation and Niutitang Formation, while the reservoir space of the Doushantuo Formation is highly heterogeneous, and

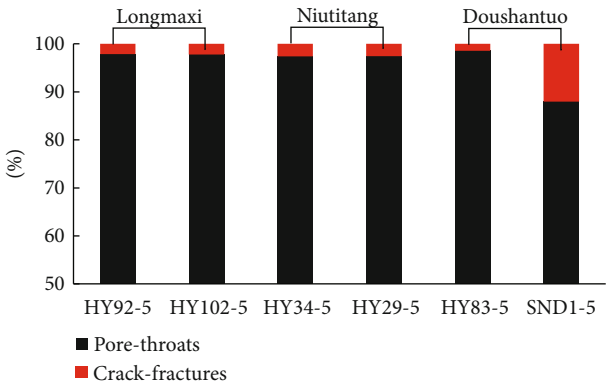

Figure 8: Pore and crack proportions in different areas.

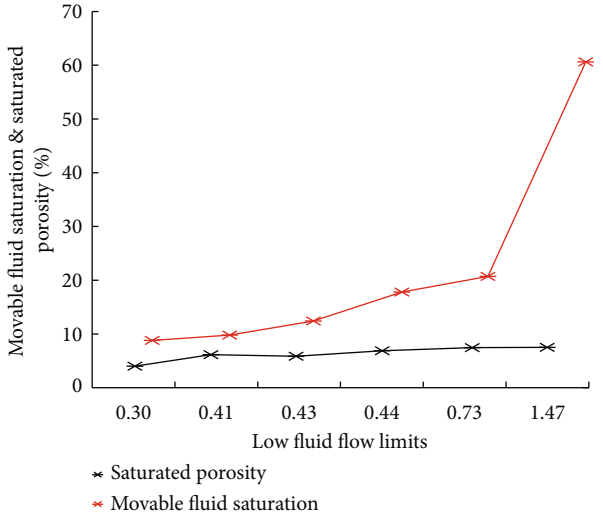

Figure 9: Evolution curves of low fluid flow limits.

some samples have many microfractures. Although the microfractures can improve the seepage capacity, the corresponding regional formation pressure is released, resulting in insufficient formation energy, which leads to a low recoverable degree and large-scale expansion of the desert location. Therefore, from the perspective of the reservoir space, the Longmaxi Formation and Niutitang Formation have advantages.

As shown in Figure 8, both the Longmaxi Formation and Doushantuo Formation are mainly of the pore type, while the no. 1 sample of the Doushantuo Formation is mainly of the pore type, and the no. 2 sample has obvious cracks. The strong heterogeneity of the pore structure in the Doushantuo Formation makes it difficult to evaluate its movable fluid. At the same time, more fractures often correspond to larger formation energy release, resulting in weak flowability.

As shown in Figure 9, based on the storage capacity and movable fluid saturation, the lower limit of the fluid flow increases with the increase of temperature. This shows that for shale reservoirs, under the same pressure conditions, a high reservoir capacity and large amount of movable fluid cannot fully correspond to a high recoverable degree. As the reservoir capacity of shale is determined by its own lower limit of the pore throat, while other reservoirs mainly depend on the upper limit of pore throat, the continuous improvement of the lower limit leads to the continuous reduction of the true recoverable degree; that is, the fluid in the pores below the lower limit cannot be discharged smoothly, affecting the final recovery rate. Therefore, attention should be paid to this problem during the reconstruction of shale reservoir. It is not allowed to only make fractures without pressurization, which will cause the fluid in the matrix to fail to break through the lower limit of pore throat, and the flowability cannot meet the expectation, resulting in a low final recovery.

5. Conclusions

(1) The provenance of the shale in the South Ordos basin was dominated by island arc volcanic rocks and some ancient fine-grained sediments. The provenances of shale in MM, HJS, and EZA may have a strong genetic relationship with the igneous rocks from the nearest HN and other volcanic rock. The provenance of the LCNF shale in the NA may comprise sediments, which are derived from the LCRS

(2) The provenance of shale tends to transit from the island arc to the continental margin from the depositional stage of USDF to LSLF. MTB inherited the tectonic evolution of the SCB, NCB, and Qinling. The igneous provenance of black shale was derived from island arcs, which is due to the weathering caused by the process of subduction and collision orogeny

(3) The high continental crust debris and deep-water environment have positive contributions to the reservoir and seepage capacity. In the sealing process of the shale reservoir, it may be counterproductive to only pursue fracture making and ignore pressurization. The capacity for a large amount of movable fluid of the shale reservoir cannot be directly equivalent to a high recoverable degree

Abbreviations

LSLF: Lower Silurian Longmaxi Formation
LCNF: Lower Cambrian Niutitang Formation
USDF: Upper Sinian Doushantuo Formation
MTB: Micangshan tectonic belt
QOB: Qinling orogenic belt
TE: Trace elements
REE: Rare earth elements
SCB: South China block
NCB: North China block
NA: Ningqiang area
HJS: Huijunba syncline
MM: Micangshan massif
EZA: Eastern Zhenba area
HN: Hannan massif
LCRS: Longmenshan continental rift system.

Data Availability

The data of this study are all included within the article.

Conflicts of Interest

The authors declare that the research was conducted in the absence of any commercial or financial relationships that could be construed as a potential conflict of interest.

Acknowledgments

The authors are appreciative of the anonymous coresearchers from Nanjing University for their valuable advice. This study was supported by the Key Project of Shaanxi Coal Geology Group Co., Ltd. (SMDZ (KY)-2020-004); the Independent Project of the Key Laboratory of Coal Exploration and Comprehensive Utilization, MNR (KF2019-2, KF2021-3, and KF2020-2); and the National Natural Science Foundation of China (51874240 and 51934005).

Supplementary Materials

The supplementary material for this article has provide the element results in different research areas. Table S1: the element results in Longmaxi shale in eastern Micangshan. Table S2: the element results in Longmaxi shale in northeast Micangshan. Table S3: the element results in Niutitang shale in eastern Micangshan. Table S4: the element results in Niutitang shale in Huijunba. Table S5: the element results in Niutitang shale in northeast Micangshan. Table S6: the element results in Niutitang shale in Ningqiang. Table S7: the element results in Niutitang shale in eastern Zhenba. Table S8: the element results in Doushantuo shale in eastern Zhenba. *(Supplementary Materials)*

References

[1] Z. Caineng, D. Dazhong, W. Yuman et al., "Shale gas in China: characteristics, challenges and prospects (I)," *Petroleum Exploration and Development*, vol. 42, no. 6, pp. 753–767, 2015.

[2] C. Zou, D. Dong, Y. Wang et al., "Shale gas in China: characteristics, challenges and prospects (II)," *Petroleum Exploration and Development*, vol. 43, no. 2, pp. 182–196, 2016.

[3] L. Zhang, X. He, X. Li et al., "Shale gas exploration and development in the Sichuan Basin: progress, challenge and countermeasures," *Natural Gas Industry*, vol. 9, pp. 176–186, 2022.

[4] Y. Dong and M. Santosh, "Tectonic architecture and multiple orogeny of the Qinling Orogenic Belt, Central China," *Gondwana Research*, vol. 29, no. 1, pp. 1–40, 2016.

[5] D. L. T. T. Fu, J. Q. Qin, F. Yang, Y. H. Han, and Y. F. Qian, "Characterization of methane adsorption on the shales in Niutitang Formation at Dazhuba-Huijunba Oblique," *Journal of China Coal Society*, vol. 43, no. 12, pp. 3453–3460, 2018.

[6] T. Tian, S. Zhou, D. Fu, F. Yang, and J. Li, "Characterization and controlling factors of pores in the Lower Cambrian Niutitang shale of the Micangshan tectonic zone, SW China," *Arabian Journal of Geosciences*, vol. 12, no. 7, pp. 1–14, 2019.

[7] T. Tian, S. Zhou, D. Fu, F. Yang, and J. Li, "Calculation of the original abundance of organic matter at high-over maturity: a case study of the Lower Cambrian Niutitang shale in the Micangshan-Hannan Uplift, SW China," *Journal of Petroleum Science and Engineering*, vol. 179, pp. 645–654, 2019.

[8] E. E. Bokanda, P. Fralick, E. Ekomane et al., "Geochemical constraints on the provenance, paleoweathering and maturity of the Mamfe black shales, West Africa," *Journal of African Earth Sciences*, vol. 175, article 104078, 2021.

[9] Y. C. J. Wang, L. Hu, and Y. M. Zhu, "Sedimentary environment control on shale gas reservoir: a case study of Lower Cambrian Qiongzhusi Formation in the Middle Lower Yangtze area," *Journal of China Coal Society*, vol. 38, no. 5, pp. 845–850, 2013.

[10] R. G. Loucks and S. C. Ruppel, "Mississippian Barnett shale: lithofacies and depositional setting of a deep-water shale-gas succession in the Fort Worth Basin, Texas," *AAPG Bulletin*, vol. 91, no. 4, pp. 579–601, 2007.

[11] Z. Jianhua, J. Zhijun, J. Zhenkui et al., "Lithofacies types and sedimentary environment of shale in Wufeng-Longmaxi Formation, Sichuan Basin," *Acta Petrolei Sinica*, vol. 37, no. 5, pp. 572–586, 2016.

[12] D. Liu, D. Ren, K. Du, Y. Qi, and F. Ye, "Impacts of mineral composition and pore structure on spontaneous imbibition in tight sandstone," *Journal of Petroleum Science and Engineering*, vol. 201, article 108397, 2021.

[13] D. Ren, L. Ma, D. Liu, J. Tao, X. Liu, and R. Zhang, "Control mechanism and parameter simulation of oil-water properties on spontaneous imbibition efficiency of tight sandstone reservoir," *Frontiers in Physics*, vol. 10, p. 47, 2022.

[14] H. Deng, G. Sheng, H. Zhao et al., "Integrated optimization of fracture parameters for subdivision cutting fractured horizontal wells in shale oil reservoirs," *Journal of Petroleum Science and Engineering*, vol. 212, article 110205, 2022.

[15] H. Wang, Z. Kou, D. A. Bagdonas et al., "Multiscale Petrophysical characterization and flow unit classification of the Minnelusa Eolian sandstones," *Journal of Hydrology*, vol. 607, article 127466, 2022.

[16] M. R. Bhatia, "Plate tectonics and geochemical composition of sandstones," *The Journal of Geology*, vol. 91, no. 6, pp. 611–627, 1983.

[17] K.-J. Zhang, B. Li, and Q.-G. Wei, "Diversified provenance of the Songpan-Ganzi Triassic turbidites, Central China: constraints from geochemistry and Nd isotopes," *The Journal of Geology*, vol. 120, no. 1, pp. 69–82, 2012.

[18] K.-J. Zhang, Q.-H. Li, L.-L. Yan et al., "Geochemistry of limestones deposited in various plate tectonic settings," *Earth-Science Reviews*, vol. 167, pp. 27–46, 2017.

[19] Z. Yingli, W. Zongqi, Y. Zhen, and W. Tao, "Tectonic setting of Neoproterozoic Beiyixi Formation in Quruqtagh area, Xinjiang: evidence from geochemistry of clastic rocks," *Acta Petrologica Sinica*, vol. 27, no. 6, pp. 1785–1796, 2011.

[20] D. Yan, H. Wang, Q. Fu, Z. Chen, J. He, and Z. Gao, "Geochemical characteristics in the Longmaxi Formation (Early Silurian) of South China: implications for organic matter accumulation," *Marine and Petroleum Geology*, vol. 65, pp. 290–301, 2015.

[21] A. Odoma, N. Obaje, J. Omada, S. Idakwo, and J. Erbacher, "Mineralogical, chemical composition and distribution of rare earth elements in clay-rich sediments from southeastern Nigeria," *Journal of African Earth Sciences*, vol. 102, pp. 50–60, 2015.

[22] O. I. Ejeh, "Geochemistry of rocks (Late Cretaceous) in the Anambra Basin, SE Nigeria: insights into provenance, tectonic

setting, and other Palaeo-conditions," *Heliyon*, vol. 7, no. 10, article e08110, 2021.

[23] D. Ren, X. Wang, Z. Kou et al., "Feasibility evaluation of CO2 EOR and storage in tight oil reservoirs: a demonstration project in the Ordos Basin," *Fuel*, vol. 331, article 125652, 2023.

[24] Y.-C. Tian, C.-Q. Shu, M. Xu, S. Rao, B. P. Kohn, and K.-B. Hu, "Exhumation history of the Micangshan-Hannan Dome since Cretaceous and its tectonic significance: evidences from apatite fission track analysis," *Chinese Journal of Geophysics*, vol. 53, no. 4, pp. 920–930, 2010.

[25] Z. Yang, L. Ratschbacher, R. Jonckheere et al., "Late-stage foreland growth of China's largest orogens (Qinling, Tibet): evidence from the Hannan-Micang crystalline massifs and the northern Sichuan Basin, Central China," *Lithosphere*, vol. 5, no. 4, pp. 420–437, 2013.

[26] H.-C. Shi and X.-B. Shi, "Exhumation process of Middle-Upper Yangtze since Cretaceous and its tectonic significance: low-temperature thermochronology constraints," *Chinese Journal of Geophysics*, vol. 57, no. 8, pp. 2608–2619, 2014.

[27] D. Dong, Y. Wang, X. Li et al., "Breakthrough and prospect of shale gas exploration and development in China," *Natural Gas Industry B*, vol. 3, no. 1, pp. 12–26, 2016.

[28] G. Sheng, Y. Su, and W. Wang, "A new fractal approach for describing induced-fracture porosity/permeability/ compressibility in stimulated unconventional reservoirs," *Journal of Petroleum Science and Engineering*, vol. 179, pp. 855–866, 2019.

[29] G. Weng, Q. Xie, C. Xu, P. Zhang, and X. Zhang, "Seismic response of cable-stayed spanning pipeline considering medium-pipeline fluid–solid coupling dynamic effect," *PRO*, vol. 11, no. 2, p. 313, 2023.

[30] M. R. Bhatia and K. A. Crook, "Trace element characteristics of graywackes and tectonic setting discrimination of sedimentary basins," *Contributions to Mineralogy and Petrology*, vol. 92, no. 2, pp. 181–193, 1986.

[31] K. C. Condie, "Geochemical changes in baslts and andesites across the Archean-Proterozoic boundary: identification and significance," *Lithos*, vol. 23, no. 1-2, pp. 1–18, 1989.

[32] P. Floyd and B. Leveridge, "Tectonic environment of the Devonian Gramscatho basin, South Cornwall: framework mode and geochemical evidence from turbiditic sandstones," *Journal of the Geological Society*, vol. 144, no. 4, pp. 531–542, 1987.

[33] D. J. Wronkiewicz and K. C. Condie, "Geochemistry and mineralogy of sediments from the Ventersdorp and Transvaal Supergroups, South Africa: cratonic evolution during the early Proterozoic," *Geochimica et Cosmochimica Acta*, vol. 54, no. 2, pp. 343–354, 1990.

[34] X. Gu, J. Liu, M. Zheng, J. Tang, and L. Qi, "Provenance and tectonic setting of the Proterozoic turbidites in Hunan, South China: geochemical evidence," *Journal of sedimentary Research*, vol. 72, no. 3, pp. 393–407, 2002.

[35] Y. Song, Z. Liu, Q. Meng, Y. Wang, G. Zheng, and Y. Xu, "Petrography and geochemistry characteristics of the lower Cretaceous Muling Formation from the Laoheishan Basin, Northeast China: implications for provenance and tectonic setting," *Mineralogy and Petrology*, vol. 111, no. 3, pp. 383–397, 2017.

[36] M. R. Bhatia, "Rare earth element geochemistry of Australian Paleozoic graywackes and mudrocks: provenance and tectonic control," *Sedimentary Geology*, vol. 45, no. 1-2, pp. 97–113, 1985.

[37] T. Tian, P. Yang, J. Yao et al., "New detrital apatite fission track thermochronological constraints on the Meso-Cenozoic tectono-thermal evolution of the Micangshan-Dabashan tectonic belt, Central China," *Frontiers in Earth Science*, vol. 9, article 754137, 2021.

[38] X. Gu, "Geochemical characteristics of the Triassic Tethys-turbidites in northwestern Sichuan, China: implications for provenance and interpretation of the tectonic setting," *Geochimica et Cosmochimica Acta*, vol. 58, no. 21, pp. 4615–4631, 1994.

[39] K. E. Higgs and P. R. King, "Sandstone provenance and sediment dispersal in a complex tectonic setting: Taranaki Basin, New Zealand," *Sedimentary Geology*, vol. 372, pp. 112–139, 2018.

[40] J. He and X. Yao, "From an individual to a population: an analysis of the first hitting time of population-based evolutionary algorithms," *IEEE Transactions on Evolutionary Computation*, vol. 6, no. 5, pp. 495–511, 2002.

[41] Y. Zheng and S. Zhang, "Formation and evolution of Precambrian continental crust in South China," *Chinese Science Bulletin*, vol. 52, no. 1, pp. 1–12, 2007.

[42] S. Li, G. Zhang, L. Zhou et al., "The opposite Meso-Cenozoic intracontinental deformations under the superconvergence: rifting and extension in the North China craton and shortening and thrusting in the South China craton," *Earth Science Frontiers*, vol. 18, no. 3, pp. 79–107, 2011.

[43] J.-H. Zhao and M.-F. Zhou, "Neoproterozoic adakitic plutons in the northern margin of the Yangtze block, China: partial melting of a thickened lower crust and implications for secular crustal evolution," *Lithos*, vol. 104, no. 1-4, pp. 231–248, 2008.